

High Thermal Stability Is Essential for Tumor Targeting of Antibody Fragments: Engineering of a Humanized Anti-epithelial Glycoprotein-2 (Epithelial Cell Adhesion Molecule) Single-Chain Fv Fragment¹

Jörg Willuda, Annemarie Honegger, Robert Waibel, P. August Schubiger, Rolf Stahel, Uwe Zangemeister-Wittke, and Andreas Plückthun²

Department of Biochemistry, University of Zürich, CH-8057 Zürich, Switzerland [J. W., A. H., A. P.]; Division of Oncology, Department of Internal Medicine, University Hospital, CH-8044 Zürich, Switzerland [J. W., R. S., U. Z.-W.]; and Center for Radiopharmaceutical Science, Paul Scherrer Institute, CH-5232 Villigen (PSI), Switzerland [R. W., P. A. S.]

ABSTRACT

The epithelial glycoprotein-2 is abundantly expressed on many solid tumors and is a suitable target for antibody-based therapy. In the present study, an anti-epithelial glycoprotein-2 single-chain Fv (scFv) was derived from the hybridoma MOC31 by phage display. Despite its high affinity ($K_D = 3.9 \times 10^{-9}$ M), however, this antibody fragment failed to significantly enrich at lung tumor xenografts in mice, mostly because of its insufficient thermal stability. To overcome this limitation, the antigen-binding residues of the MOC31 scFv fragment were grafted onto the framework of the highly stable and well-folding anti-*c-erbB2* scFv 4D5. Further modification of the resulting 4D5 MOC-A, which was performed by transferring eight additional residues of the heavy chain variable domain core of the parent MOC31 antibody, produced 4D5 MOC-B, resulting in increased serum stability at 37°C and also significantly improved expression behavior while retaining the antigen specificity and affinity of the parent MOC31 scFv. In mice, the scFv 4D5 MOC-B, which was radiolabeled with ^{99m}technetium using a new histidine-tag specific labeling method (Waibel *et al.*, *Nature Biotechnol.*, 17: 897–901, 1999), showed favorable blood clearance and efficient enriches at lung tumor xenografts, with a tumor:blood ratio of 5.25 and a total dose of 1.47% injected dose per gram after 24 h. Biophysical properties such as high thermal stability are thus decisive for whether these molecules are useful *in vivo*, and our approach may provide a general strategy to solve this problem. This is also the first report of using a humanized anti-EGP-2 scFv *in vivo* for targeting solid tumors, which is a promising targeting moiety for the diagnostics and therapy of EGP-2-positive tumors in patients.

INTRODUCTION

The mAb³ MOC31 recognizes the 38-kDa transmembrane EGP-2 (also known as GA733–2, an epithelial cell adhesion molecule, or an adenocarcinoma-associated KS1/4 antigen; Ref. 1). EGP-2 is a promising tumor-associated antigen for imaging and therapy due to its abundant expression in a variety of solid tumors. Recent clinical studies could prove the usefulness of anti-EGP2 mAbs such as 17–1A (Panorex) and MOC31 for therapy and diagnostics in patients with colon and lung cancer (2–4). In a recent study, we could demonstrate the ability of an immunotoxin consisting of *Pseudomonas* exotoxin A chemically linked to MOC31 to inhibit the growth of small lung tumor xenografts in athymic mice (5). Although the precise function of the transmembrane glycoprotein EGP-2 is still not well understood, recent

reports have identified EGP-2 as a homophilic cell adhesion molecule (6, 7) and have suggested its role as a modulator of invasiveness and metastasis (8).

Carcinoma-associated antigens, such as *c-erbB2* (HER-2), carcino-embryonic antigen, and EGP-2 have been used as targets for radiolabeled antibodies in tumor imaging and therapy studies (4, 9–11). Efforts have been made to improve the targeting efficiency of these antibodies by reducing the molecular weight and thereby increasing their tissue penetration and serum clearance. Fab, (Fab)₂, disulfide-stabilized Fv, and scFv fragments of antibodies generated by recombinant technology hold great promise in this regard (9, 12). However, the optimal functional parameters of these molecules, such as required stability, optimal molecular weight, and required affinity are poorly understood and have to be optimized depending on the diverse clinical requirements (13).

scFv fragments consist of the variable domains of the heavy and light chain connected by a flexible peptide linker (14, 15). Fv fragments and linked derivatives conserve the monovalent binding affinity and the specificity of the parent mAb and can be produced in bacteria (16). They can be constructed by cloning the variable domains of mAbs from hybridoma cells or by direct selection of scFv fragments with the desired specificity from immunized or naive phage libraries (17–19). scFv fragments, whether cloned from hybridomas or obtained from phage libraries, can show poor production yields and exhibit low thermodynamic stability, thereby limiting their usefulness for *in vivo* applications, even if they have excellent affinities and specificities (20). Recombinant antibody fragments that have been obtained by either strategy may thus have very valuable properties in terms of epitope and specificity, but their biophysical behavior leaves much to be desired.

One possibility to “repair” such scFv fragments with suboptimal stability and/or folding yield is the grafting of their CDRs onto the framework of a different, more stable scFv. This was shown for the fluorescein binding antibody fragment 4–4–20 of which the CDRs were grafted on the hu4D5-framework (simply denoted here by “4D5”), leading to a significant improvement of both expression yield and thermodynamic stability (21). The 4D5 framework itself is an artificial framework derived from human consensus sequences, which essentially corresponds to the germ-line sequences, IGVH 3–66 and IGVK 1–39 (IMGT nomenclature)⁴ and was originally used for the humanization of the anti-*c-erbB2* (p185^{HER2}-ECD) mAb 4D5 (Herceptin; Ref. 22). The good expression yield of various constructs of 4D5 in *Escherichia coli* (23) and the above-average thermodynamic stability have been described (24).

In the present study, we report the improvement of an unstable high-affinity anti-EGP-2 scFv fragment cloned from the hybridoma MOC31, which failed to significantly enrich at tumor xenografts despite its high affinity, by grafting its binding residues onto the framework of the scFv 4D5 and by further identification and intro-

Received 5/28/99; accepted 9/22/99.

The costs of publication of this article were defrayed in part by the payment of page charges. This article must therefore be hereby marked *advertisement* in accordance with 18 U.S.C. Section 1734 solely to indicate this fact.

¹ This work was supported by Grant 161-9-1995 from Krebsforschung Schweiz.

² To whom requests for reprints should be addressed, at Department of Biochemistry, University of Zürich, Winterthurerstrasse 190, CH-8057 Zürich, Switzerland. Phone: 41-1-635-5570; Fax: 41-1-635-5712; E-mail: plueckthun@biocfebs.unizh.ch.

³ The abbreviations used are: mAb, monoclonal antibody; CDR, complementarity determining region; ECD, extracellular domain; EGP-2, epithelial glycoprotein-2; ID/g, injected dose per gram; IMAC, immobilized metal ion affinity chromatography; IMGT, immunogenetics database, Montpellier; PDB, Brookhaven protein database; scFv, single-chain Fv; ^{99m}Tc, ^{99m}technetium; V_H, heavy chain variable domain; V_L, light chain variable domain; RIA, radio-immunoassay.

⁴ Tomlinson, I. <http://www.mrc-cpe.cam.ac.uk/imt-doc>. (MRC Centre for Protein Engineering, Hills Road, Cambridge CB2 2QH, United Kingdom), 1999.

duction of stabilizing framework residues. This modification resulted in a functionally improved humanized anti-EGP-2 scFv of which for the first time, tumor localization data in athymic mice are presented. Our results clearly demonstrate the decisive importance of the biophysical properties of scFv fragments for effective targeting of tumors *in vivo* and provide general guidelines for the engineering of such molecules.

MATERIALS AND METHODS

Mammalian Cell Lines. The human small cell lung carcinoma cell line SW2 (kindly provided by Dr. S. D. Bernal, Dana-Farber Cancer Institute, Boston, MA) and the breast carcinoma cell line SK-BR-3 (#HTB 30, American Type Culture Collection, Rockville, MD) were maintained in RPMI 1640 medium (Hyclone, Europe Ltd.) supplemented with 10% bovine serum (Life Technologies, Inc., Grand Island, NY) and grown at 37°C in an atmosphere of 5% CO₂. The breast carcinoma cell line SK-OV-3 (#HTB 77, American Type Culture Collection, Rockville, MD) was grown in RPMI 1640 medium supplemented with 10% bovine serum, EGF (10 ng/ml), and insulin (5 ng/ml).

Soluble EGP-2 and scFv Fragments. A 788-bp *XhoI/EcoRI* fragment containing the ECD of EGP-2 (Met1-PHE259) was subcloned into pBlue-BAC4 (Invitrogen, de Schelp, NL), and a small *EcoRI/SalI* linker-adapter encoding a hexahistidine-tag was subcloned downstream from the EGP-2 coding sequence. Expression in a baculovirus system and purification of EGP-2 was performed as described before (25). The anti-EGP-2 scFv fragment (scFv MOC31) was assembled from mRNA isolated from the murine hybridoma cell line MOC31 (1) by use of a reengineered phage display system as described (19). The scFv fragment from the human anti-*c-erbB2* antibody 4D5 was constructed from the Fab fragment (22) and was used in several studies before (24, 26).

Molecular Modeling and Construction of Loop Graft. A homology model of the anti-EGP-2 scFv fragment was generated using the molecular modeling software Insight97 (Biosym/MSI, Modules Homology, Biopolymer, and Discover). The V_L domain model was based on the X-ray structures of the mouse Fab fragment JEL103 (Ref. 27; PDB entries 1mrc, 1mrd, 1mre, and 1mrf; 2.3 Å–2.4 Å resolution; 76% sequence identity to MOC31); the V_H domain model was based on the structure of an antineuraminidase Fab [Ref. 28, 29; PDB entries 1nca, 1ncb, 1ncc, and 1ncd (Ref.30); 2.5 Å resolution; 85% identity] and the CDR H3 conformation of the anticholera toxin Fab TE33 [Ref. 31; PDB entry 1tet (32); 2.3 Å resolution; 82% identity]. The MOC31 domain models were superimposed on the crystal structure of the Fv of humanized 4D5 version 8 (Ref. 33; PDB entry 1fvc; 2.2 Å resolution; V_L: 55% identity; V_H: 50% identity to MOC31). Potential antigen contacts were identified by comparing the side chain solvent-accessible surface of known antibody-protein complexes in the presence and absence of the ligand using the program NACCESS⁵. The models were checked for possible steric conflicts, potential antigen contacts, and residues that might have an indirect influence on CDR conformations, which might result in the hybrid scFv 4D5 MOC-A. In a second construct, scFv 4D5 MOC-B, eight key residues in the core of V_H were retained from the MOC31 sequence instead of changing them to the 4D5 sequence to preserve the structural subtype of the MOC31 V_H framework (see “Results”).

The designed sequences for both variants were back-translated (GCG-package), and the fragments were constructed by gene synthesis (34) from eight overlapping oligonucleotides for V_L and ten for the two different variants of V_H in the orientation V_L-linker-V_H. The length of the oligonucleotides used was between 40 bp and 78 bp. Each domain was produced separately, cloned blunt-ended into the vector pBluescript (Stratagene), and sequenced. V_L and V_H domains were then cloned into the expression vector pIG6 (35). A 24-mer nonrepetitive linker T_{PSHNSHQVPSAGGPTANS}GTSGS (36) was introduced by cassette mutagenesis.

Expression and Purification of scFv Fragments. For periplasmic expression of the *c-erbB2* binding scFv fragment 4D5 and the EGP-2 binding scFv fragments, 4D5 MOC-A and 4D5 MOC-B, the vector pIG6 (35) was used, whereas the vector pAK400 (19) was used for the expression of scFv MOC31. For large-scale production, the *E. coli* strain SB536 (37) was used. One liter of

2YT containing 1% glucose and ampicillin (30 μg/ml) in a 5-liter shake flask was inoculated with 30 ml of overnight culture. When the culture reached an A_{550 nm} of 0.5, scFv production was induced with a final concentration of 1 mM isopropyl-D-galactopyranoside (IPTG; Boehringer Mannheim) for 3–4 h at 24°C. The final absorbance was 5–6 for 4D5, 4D5 MOC-A, and 4D5 MOC-B and 4 for scFv MOC31. The harvested pellet was stored at –80°C.

For purification, the pellet from 1 liter of culture was resuspended in 20 mM Hepes (pH 7.0) and 30 mM NaCl and lysed with two cycles in a French Pressure Cell press (SLS Instruments, Urbana, IL). The cleared lysate was centrifuged in a SS-34 rotor at 48,000 g at 4°C and filter-sterilized. All scFv fragments were purified over a Ni²⁺-IDA-column and HS/M-4.6/100-ion-exchange column and coupled in-line on a BIOCAD-System (Perceptive BioSystems) as described previously (38). After loading the lysate on the Ni²⁺-IDA column, the column was washed with 20 mM Hepes (pH 7.0), 500 mM NaCl, and in a second step with 20 mM Hepes (pH 7.0), 40 mM imidazole before the bound protein was eluted with 200 mM imidazole (pH 7.0). The eluate was loaded directly on the HS/M-4.6/100-ion-exchange column, and the specifically bound protein was eluted with a salt gradient of 0–500 mM NaCl in 20 mM Hepes (pH 7.0). The fraction containing the antibody fragment was dialyzed against an excess of PBS and concentrated to 1 mg/ml using a 10 kDa cutoff filter (Ultrafree-MC low protein binding, Millipore) by centrifugation at 4000 g at 4°C. For the anti-EGP-2 scFv fragment MOC31, it was necessary to perform a preparative gel filtration with a Superdex-75 column (Pharmacia) as the third purification step. The result of the purification was checked on a 12.5% SDS-PAGE under reducing and nonreducing conditions. The molecular weights of all purified scFv fragments were checked by mass spectrometry.

His-Tag Specific ^{99m}Tc Labeling of scFv Fragments. For ^{99m}Tc labeling, the His-tag-specific ^{99m}Tc labeling method was used as described (39). ^{99m}Tc-tricarbonyl trihydrate forms very stable complexes with the penta- or hexahistidine tag, allowing the dual use of the His-tag for IMAC and labeling. The scFv fragments (1 mg/ml) were mixed with one-third of the volume of the ^{99m}Tc-tricarbonyl reaction mixture (30 mCi/ml) and incubated for 30 min at 37°C. scFv MOC31 was labeled for 30 min at 30°C at a protein concentration of 400 μg/ml to avoid precipitation. The reaction mixture was desalted over a FAST-desalting column (Pharmacia) equilibrated with PBS. Aliquots of the collected fractions were counted by γ-scintillation to identify the fractions containing labeled protein.

Analytical Gel Filtration. Analytical gel filtrations were performed with the Smart system (Pharmacia) using a Superdex-75 column. All measurements were performed in PBS containing 0.005% Tween 20. The scFv fragments were injected at a concentration of 200 μg/ml for scFv MOC31 and of 1 mg/ml for 4D5 MOC-A and 4D5 MOC-B in a volume of 15 μl before and after overnight incubation for 20 h at 37°C. The column was calibrated in the same buffer with alcohol dehydrogenase (*M_r* 150,000), BSA (*M_r* 66,000), carbonic anhydrase (*M_r* 29,000), and cytochrome *c* (*M_r* 12,400) as molecular weight standards.

Binding Specificity. The binding specificity of the different scFv fragments was tested by competition binding with the mAb MOC31. Fifty nanograms of radiolabeled scFv 4D5 MOC-A or 4D5 MOC-B were incubated with SW2 cells (0.5 × 10⁶) in 200 μl of PBS/1% BSA after preincubation with or without the mAb MOC31 (10 μg) or with the same amount of an anti-*c-erbB2* mAb as an irrelevant competitor for 30 min at 4°C. In three washing steps, cells were centrifuged at 1000 g for 5 min at 4°C, the supernatant was discarded, and the cells were resuspended in PBS/1% BSA. The remaining radioactivity was then counted by γ-scintillation. In a further binding experiment, both scFv fragments (50 ng) were incubated with different antigens coated (500 ng/well) on a 96-well microtiter plate to check for cross-reactivity. The wells were washed three times with PBS/1% BSA, and the radioactivity was determined.

K_D-Determination by RIA and Surface Plasmon Resonance (BIAcore). The binding affinity of the ^{99m}Tc-labeled scFv fragments was estimated on SW2 cells in an RIA. SW2 cells (0.5 × 10⁶) were incubated with increasing amounts of the scFv fragment (100 pM–30 nM) for 1 h at 4°C. For the estimation of nonspecific binding, control samples of cells were preincubated with a 100-fold excess of an unlabeled scFv fragment for 1 h at 4°C. The bound fraction of the scFv fragments was determined in a scintillation counter. Each value represents the mean of two samples. Counts per minute were plotted against the concentration of the scFv fragment, and data were fitted by using the approximate function $y = y_{\max} \times x / (K_D + x)$, where x is the concentration

⁵ Hubbard, S., and Thornton, J. <http://sjh.bi.umist.ac.uk/naccess.html>, 1992.

of radioligand, y is the radioactivity attributable to specific binding, and y_{\max} is its plateau value.

Association and dissociation rate constants were determined by surface plasmon resonance (BIAcore) with a BIAcore instrument (Pharmacia). A recombinant soluble EGP-2-antigen was covalently coupled to a CM-5 sensor chip via free amino groups, resulting in a surface coverage of 350 resonance units. scFv fragments were injected in increasing concentrations (0.1 nM–4 μ M) at a flow rate of 30 μ l/min of degassed PBS/0.005% Tween 20. Association and dissociation rate constants were calculated from the sensorgram by a global curve fit using the BIAevaluation 3.0 software (Pharmacia).

Serum Stability of Radiolabeled scFv at 37°C. The fraction of scFv fragments remaining immunoreactive after radioactive labeling was determined as described by Lindmo *et al.* (40). Samples containing increasing numbers of cells (0.625×10^6 – 10×10^6) in 100 μ l were incubated with 50 ng of radiolabeled scFv fragments for 1 h at 4°C on a shaker. Nonspecific binding was determined on control samples of cells preincubated with a 100-fold excess of unlabeled scFv fragments in PBS/1% BSA. After incubation, the cells were washed three times with PBS/1% BSA. The bound activity in the cell pellets was counted by gamma scintillation (40). To estimate the stability of the different radiolabeled scFv fragments in serum, the molecules were incubated overnight (20 h) in human serum at 37°C at a final concentration of 17 μ g/ml, and the remaining immunoreactivity was determined.

Blood Clearance and Tumor Localization. Blood clearance and biodistribution studies of scFv were performed in 6–8-week old female CD1 and BALB/c athymic mice. For blood clearance studies, each mouse received i.v. injections of 300 μ Ci of ^{99m}Tc -labeled scFv fragment 4D5 MOC-B. After 7.5, 15, 30, 60, 120, and 240 min after injection, blood samples were taken, and the $t_{1/2\alpha}$ and $t_{1/2\beta}$ values were calculated from the measured radioactivity. Biodistribution analysis of the ^{99m}Tc -labeled scFv fragments MOC31, 4D5 MOC-A, and 4D5 MOC-B were performed in mice bearing SW2 tumor xenografts of 40–80 mg in size. Each mouse received 5–30 μ g (300 μ Ci) of a ^{99m}Tc -labeled scFv fragment (purity >95%). Antifluorescein-binding scFv FITC-E2 (18) was used as a nonspecific control antibody. Mice were killed at 1, 4, and 24 h after injection, and tissue and organs were removed and assessed for activity using a gamma counter.

RESULTS

Molecular Modeling and Construction of Loop Graft. We have constructed the scFv fragment of MOC31 from the hybridoma using standard phage display methodology (19), determined its functionality, and found a rather high affinity of about 3×10^{-9} M to its antigen EGP-2 (Table 1). This scFv fragment had the same variable domain sequence as an scFv fragment independently constructed from the hybridoma MOC31, and the experimentally determined affinity was also very similar (41). The *in vivo* localization of this “natural” scFv was hardly distinguishable from a control scFv without EGP-2 specificity, and we had to conclude that the scFv MOC31 did not sufficiently enrich at a SW2 lung tumor xenograft (Table 2). We therefore hypothesized that this protein was not stable enough and designed two further variants with improved stability. The first was obtained by grafting the loops to a well-characterized stable framework, and the second was constructed by additionally changing several residues in the interior of one of the variable domains. As the recipient frame-

Table 2 Biodistribution of ^{99m}Tc -labeled scFv fragments in athymic mice bearing SW2 tumor xenografts

Organs	ScFv MOC31			FITC-E2
	1 h (n = 3)	4 h (n = 3)	24 h (n = 3)	24 h (n = 3)
Blood	ID/g ^a 8.46 \pm 0.87	ID/g 5.55 \pm 1.98	ID/g 1.34 \pm 0.15	ID/g 0.5 \pm 0.13
Heart	5.1 \pm 0.34	5.32 \pm 1.36	1.39 \pm 0.25	0.47 \pm 0.23
Lung	7.37 \pm 0.95	7.14 \pm 1.61	2.09 \pm 0.5	0.58 \pm 0.16
Spleen	14.86 \pm 1.91	17.84 \pm 2.77	7.6 \pm 0.56	1.2 \pm 0.09
Kidney	253 \pm 10	263 \pm 43	117 \pm 12	224 \pm 40
Stomach	4.71 \pm 1.04	4.08 \pm 1.04	1.28 \pm 0.21	0.25 \pm 0.14
Intestine	5.85 \pm 0.34	5.4 \pm 1.97	1.56 \pm 0.07	0.34 \pm 0.04
Liver	35.03 \pm 0.86	44.8 \pm 9.54	20.38 \pm 3.44	4.44 \pm 0.65
Muscle	1.64 \pm 0.23	1.57 \pm 0.36	0.75 \pm 0.82	0.31 \pm 0.15
Bone	5.97 \pm 0.41	6.01 \pm 1.71	2.04 \pm 0.68	0.57 \pm 0.3
Tumor	2.46 \pm 0.88	3.97 \pm 1.07	1.24 \pm 0.74	0.4 \pm 0.2
Tumor:blood ratio ^b	0.29	0.71	0.92	1.35

^a Biodistribution of ^{99m}Tc -labeled scFv MOC31 and FITC-E2 was studied in athymic mice bearing SW2 tumors of 40–80 mg in size after i.v. injection of the radiolabeled antibodies. Data are expressed as the mean \pm SE.

^b The ratios presented are the averages of the tumor:blood ratios for the individual mice.

work, we selected the humanized version of 4D5, which itself was derived by loop grafting (22). The 4D5 framework consists of a V_H essentially identical to the germ-line IGHV 3–66 (IMGT nomenclature; Ref. 42), or VH 3–18 (Vbase nomenclature),⁴ locus DP 3–66 (DP-86), and the κV_L derived from germ-line IGKV 1–39 (IMGT nomenclature; Ref. 42), or $V\kappa$ 1–1 (Vbase nomenclature),⁴ locus DP O12.

A homology model of MOC31 was built and compared to the X-ray structure of the human 4D5 version 8 Fv fragment (PDB entry 1fvc). Potential antigen contact residues were identified by an analysis of antibody-protein antigen complexes in the PDB (Fig. 1A). Based on this structural information rather than on Kabat definitions of CDRs, the decision was based on which residues to take from the 4D5 framework and which ones to take from the MOC31 sequence. Thus, the resulting graft did not strictly follow the CDR definition according to Kabat *et al.* (43) or Chothia *et al.* (44), but two residues (L64 and L66) were included from the CDR donor, which determine the conformation of the “outer loop” of V_L (residues L66–L71). The tip of this loop was shown to contact the antigen in some complexes, and an influence of this loop on the conformation of CDR L1 could not be excluded. Residue L66 is usually Gly in κ light chains and assumes a positive ϕ angle. If this residue is replaced by a non-Gly residue (Arg in 4D5), the outer loop assumes a different conformation, bending away from the domain. In V_H , in addition to CDR H1, residues H27–H30 were included, whereas some residues at the base of CDR2 were omitted (H62 and H63) despite being (according to CDR definitions) part of CDR H2 (43, 44), but several residues in the “outer loop” of V_H , which are sometimes referred to as CDR4, were included (residues H69, H71, H75–H77), resulting in the construct 4D5 MOC-A (Fig. 1A).

Analysis of the conformations of V_H domain frameworks revealed that these can be classified according to their framework conformation into four distinct subgroups. The conformational differences are most noticeable in framework I, particularly in positions H7–H10, although correlated sequence and conformational differences are found throughout the molecules, involving several core residues (45). These conformational changes are probably caused by the different hydrogen bonding patterns, which the fully buried Glu H6 (as in 4D5) or Gln H6 (as in MOC31) establishes in the core of the domain and are further influenced by the nature of residue H9 (Pro, Gly, or other residues; Ref. 46)⁶. Saul and Poljak (45) reported correlated structural

Table 1 Comparison of binding affinities and kinetic rate constants of scFv fragments

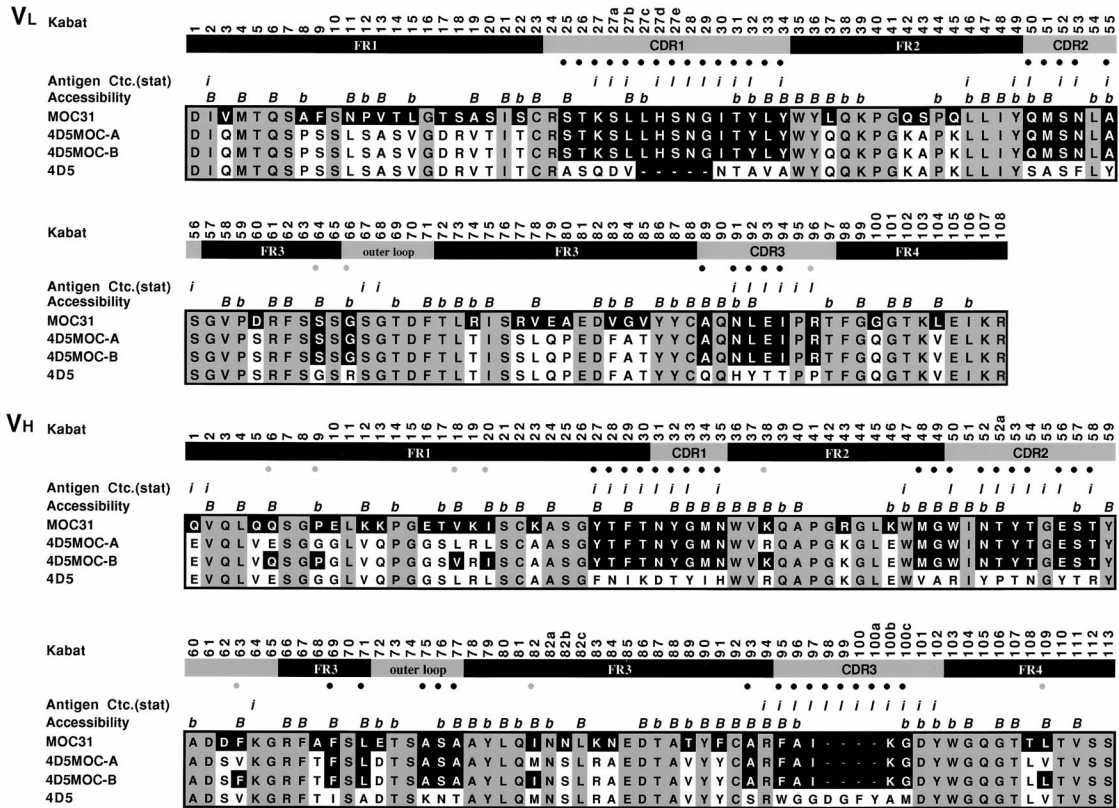
scFv	RIA ^a		Surface Plasmon Resonance ^b	
	K_D (nM) (4°C)	K_D (nM) (20°C)	k_{on} ($10^5 \text{ M}^{-1} \text{ s}^{-1}$)	k_{off} (10^{-3} s^{-1})
scFv MOC31	10.8 \pm 2.6	3.0	0.99	0.3
4D5MOC-A	3.6 \pm 0.5	3.5	1.29	0.45
4D5MOC-B	3.7 \pm 0.5	3.9	1.84	0.72

^a Interactions of purified scFv fragments with EGP-2 were determined on SW2 cells by RIA.

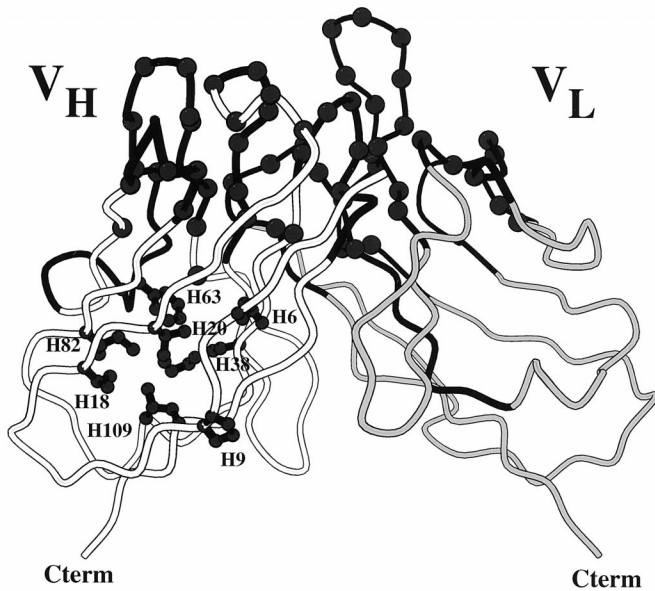
^b Interactions of purified scFv fragments with EGP-2 were also determined on immobilized EGP-2 (ECD) in real time by surface plasmon resonance (see “Materials and Methods”).

⁶ Honegger *et al.*, manuscript in preparation.

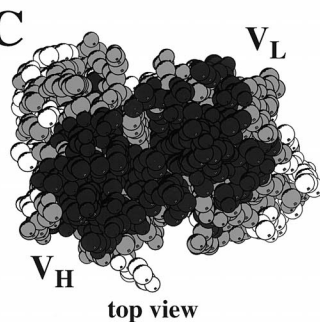
A



B



C



D

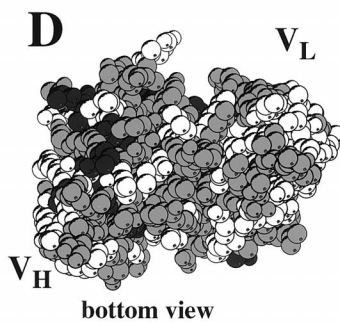


Fig. 1. A, sequence alignment of the V_L and V_H domains of scFv MOC31, 4D5 MOC-A, 4D5 MOC-B, and 4D5. Positions of sequence agreement between MOC31 and 4D5 are indicated by black letters on a gray background, residues that agree with 4D5 but are different from MOC31 are indicated by black letters on a white background, and residues that agree with MOC31 but not with 4D5 are indicated by white letters on a black background. Residue labels and CDR definitions are according to Kabat (1987). In the line "Accessibility," B indicates residues buried in the domain core or interface, and b indicates semiburied residues. In the line "Antigen Ctc (stat.)," (antigen contacts from statistics), potential antigen contact residues are indicated, and they are averaged over all protein-antibody complexes in the PDB. I denotes >40%, and i denotes a >1% loss of side chain solvent accessible surface area upon complex formation. (●), indicates residues that retain the MOC31 sequence in construct 4D5 MOC-A. (○), indicates the additional residues retaining the MOC31 sequence in construct 4D5 MOC-B. B, model of the scFv fragment 4D5 MOC-B, which is a three-dimensional structure of the anti-EGP-2 scFv fragment 4D5 MOC-B composed of V_L (gray) and V_H (white) with transferred potential antigen contact residues of MOC31 (black). The eight additional transferred murine residues in the core of V_H are indicated by black side chains. A space-filling model shows 4D5 MOC-B viewed from the top (antigen binding site; C) and from the bottom (D). Gray balls indicate residues identical in 4D5 and MOC31, black balls indicate residues that retain the murine sequence of MOC31, and white balls indicate residues changed to the 4D5 sequence.

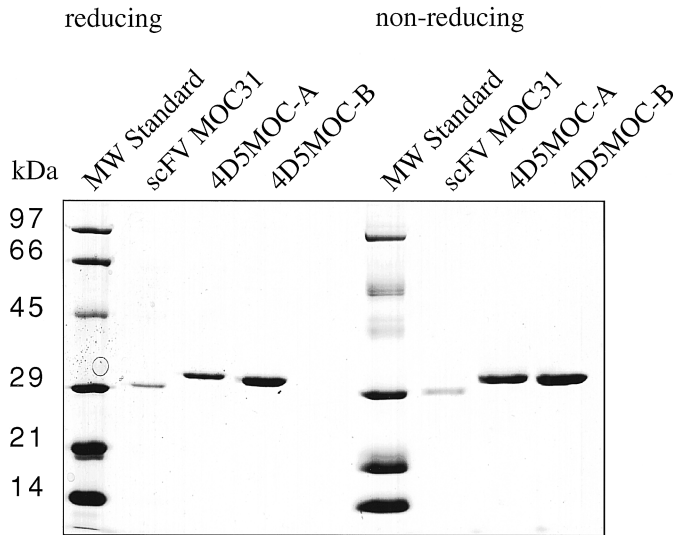


Fig. 2. Purity of scFv MOC31, scFv 4D5 MOC-A, and 4D5 MOC-B preparation. SDS-PAGE under reducing and nonreducing conditions shows the result of the purification of scFv MOC31 after IMAC, ion exchange, and gel filtration and of scFv 4D5 MOC-A and 4D5 MOC-B after IMAC and subsequent ion-exchange chromatography. Molecular weight standards: phosphorylase b (M_r 97,400), BSA (M_r 66,000), ovalbumin (M_r 44,000), carbonic anhydrase (M_r 29,000), trypsin inhibitor (M_r 21,500), and lysozyme (M_r 14,300).

changes affecting residues H9, H18, H82, H67, and H63, which relay the effects of changes in framework 1 conformation across the domain core to the base of CDR2, thus potentially enabling them to affect antigen binding.

According to this classification, MOC31 belongs to a different subclass than 4D5. Because we did not know to what extent these framework classes affect the functionality of a loop graft, we decided to test this aspect experimentally. While in construct, 4D5 MOC-A, the V_H domain framework, was changed to the 4D5 subtype, and 4D5 MOC-B fully retained the MOC31 core packing as well as the conformationally critical residues, H6 and H9.⁶ To achieve this, eight additional framework residues of the anti-EGP-2 scFv fragment sequence (H6, H9, H18, H20, H38, H63, H82, and H109) had to be taken from the MOC31 sequence. All of these changes are located in the lower half of the scFv (Fig. 1), and with the exception of the Gly-to-Pro substitution in position H9, are buried in the core of the domain. They are therefore not expected to affect the immunogenicity of the construct. For the introduction of the *Afl*III restriction site, it was necessary to modify the COOH-terminal sequence of the V_L -domain in all constructs from EIKRA to ELKRA, which was not expected to affect the domain structure.

Expression and Purification of scFv Constructs. For scFv 4D5, usually 1–2 mg of pure protein could be obtained from 1 liter of standard *E. coli* shaking culture, whereas scFv MOC31 yielded only 200 μ g of about 70% purity. Coexpression of Skp (47) increased the total yield to 600 μ g with the same degree of purity. The remaining 30% of the total protein was a proteolytic fragment of scFv MOC31 of about 20 kDa, which could be detected with an anti-His-tag antibody and must therefore contain the COOH-terminus (data not shown). This contaminant was removed by gel filtration as the third purification step, which lowered the final yield 5–10 fold. The protein used in tumor localization experiments was thus about 95% pure, and the highest concentration reached for scFv MOC31 was 400 μ g/ml. The graft variant scFv 4D5 MOC-A could be purified to a yield of 400 μ g/liter and 4D5 MOC-B to 1 mg/liter at a purity >95%. Both engineered scFv fragments could be concentrated to 1 mg/ml and were analyzed on an SDS-PAGE (Fig. 2) under reducing and nonre-

ducing conditions. Mass spectrometry of both molecules showed the expected molecular weight of M_r 28,140 for scFv MOC31, M_r 29,855 for scFv 4D5 MOC-A, and M_r 29,897 for scFv 4D5 MOC-B.

Binding Specificity. The transfer of the anti-EGP-2 binding specificity of scFv MOC31 onto the framework of scFv 4D5 was shown to be successful for both variants, 4D5 MOC-A and 4D5 MOC-B, by binding and specific competition of the radiolabeled graft variants to EGP-2 expressing SW2 cells. Only the cognate mAb MOC31 could inhibit binding of the graft variants, whereas an irrelevant control antibody did not compete (Fig. 3A). No cross-reactivity of the grafted molecules with *c-erbB2* and the EGF-receptor (ECD) were found (Fig. 3B).

Determination of K_D . High-affinity binding with a long residence time on the specific target antigen is considered to be one of the most important properties of antibodies for achieving efficient tumor tar-

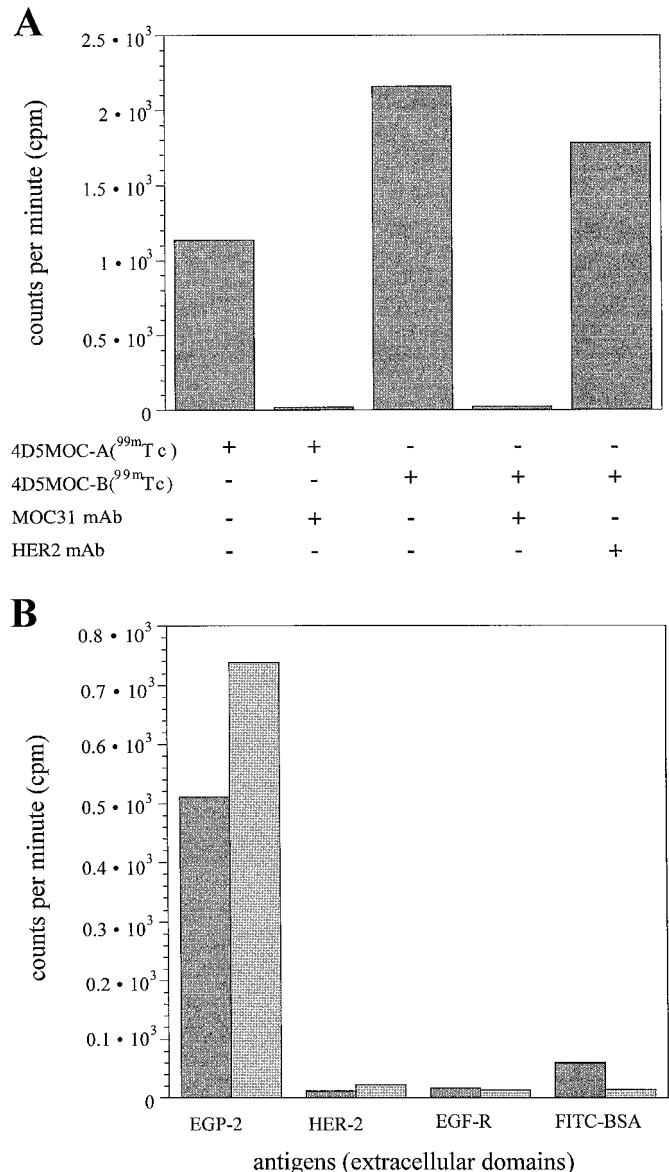


Fig. 3. Binding analysis of ^{99m}Tc-labeled 4D5 MOC-A and 4D5 MOC-B. A, competition radio-immunoassay of ^{99m}Tc-labeled 4D5 MOC-A and 4D5 MOC-B on SW2 tumor cells. Fifty-nanogram radiolabeled scFv fragments were incubated with or without unlabeled mAb MOC31 (10 μ g) or with the same amount of an irrelevant anti *c-erbB2* mAb as an irrelevant inhibitor. B, binding of ^{99m}Tc-labeled 4D5 MOC-A and 4D5 MOC-B for different soluble antigens (500 ng/well).

getting. To ensure that binding affinity was conserved in the grafting experiment, dissociation constants of the radiolabeled scFv fragments were determined on cells in an RIA. The graft variants showed similar binding behavior, which was comparable in specificity and in affinity (about 3×10^{-9} M) to the parent anti-EGP-2 scFv fragment (Table 1).

Binding kinetics of unlabeled scFv fragments to immobilized EGP-2 were also analyzed by surface plasmon resonance (Table 1) with the BIAcore instrument (Pharmacia). To minimize rebinding effects, which could lead to an underestimation of the off-rates, we used a high flow rate and quite a low coating density. The “natural” scFv MOC31 showed stable binding on its target, with a calculated half-life of about 38 min, which was consistent with an independent determination (half-life of 34 min; Ref. 41). The k_{off} values of scFv 4D5 MOC-A and 4D5 MOC-B were nearly identical to the parent scFv MOC31 (Table 1), indicating that the complete transfer of the binding properties of scFv MOC31 on the 4D5-framework was successful.

Analytical Gel Filtration and Test of Thermal Aggregation. For most experimental purposes, it is essential that scFv fragments remain stable and functional at physiological temperatures and at high concentrations. Based on this consideration, the aggregation behavior of these molecules was tested in a gel filtration assay before and after incubation at 37°C.

Almost 90% of the total protein of scFv MOC31 eluted from a Superdex-75 column at a volume of 1.27 ml, as expected for the monomeric species, whereas about 10% eluted as high molecular weight aggregates. However, ~95% of scFv MOC31 precipitated when incubated for 30 min at 37°C (Fig. 4A). The two grafted variants, 4D5 MOC-A and 4D5 MOC-B, eluted at a volume of 1.20 ml, which corresponded to a molecular weight of M_r 30,000, indicating monomers at a concentration of 1 mg/ml. Although 4D5 MOC-A precipitated more slowly than MOC31, overnight incubation in PBS at 37°C for 20 h and subsequent gel filtration showed nearly no eluted protein (Fig. 4B). In contrast, when incubated under the same conditions, 4D5 MOC-B still eluted as a symmetric peak at a volume of 1.20 ml (Fig. 4C), indicating a large difference in intrinsic (thermal) stability of the variants.

His-Tag Specific $^{99\text{m}}\text{Tc}$ Labeling. The scFv fragments were labeled with $^{99\text{m}}\text{Tc}$ by use of a new method in which $^{99\text{m}}\text{Tc}$ -tricarbonyl-trihydrate is bound to the COOH-terminal penta- or hexahistidine tag of recombinant proteins (39). The binding of the radiolabel was shown to be stable (94% remaining activity) when incubated for 24 h at 37°C in PBS with a 5000-fold molar excess of 100 mM free histidine (39). With the exception of scFv MOC31, all scFv fragments could be labeled at 37°C and at protein concentrations of 1 mg/ml, resulting in 30–40% of the initial $^{99\text{m}}\text{Tc}$ being incorporated to a final specific activity of 300–400 mCi/ml. In contrast, $^{99\text{m}}\text{Tc}$ labeling of the parent scFv MOC31 required the incubation temperature to be lowered to 30°C while the maximum protein concentration was 400 $\mu\text{g/ml}$, resulting in a markedly decreased incorporation yield (25% of total $^{99\text{m}}\text{Tc}$, 250 mCi/ml).

Determination of Immunoreactivity after Incubation in Human Serum at 37°C. Besides thermal stability, a sufficient resistance to serum proteases is also essential for the successful *in vivo* application of scFv fragments. We therefore determined the immunoreactivity of the $^{99\text{m}}\text{Tc}$ -labeled scFv fragments before (Fig. 4D) and after (Fig. 4E) incubation in human serum for 20 h at 37°C (40). For scFv MOC31, we found $67 \pm 5.4\%$ of the protein being active if the labeling reaction was performed at 30°C. The other fragments showed $47.25 \pm 4.9\%$ activity for scFv 4D5 MOC-A, $74.5 \pm 8.3\%$ for scFv 4D5 MOC-B, and $87.3 \pm 6.4\%$ for scFv 4D5, all labeled at 37°C. To test for serum stability, the scFv fragments (17 $\mu\text{g/ml}$) were incubated in human serum at 37°C for 20 h, and the remaining immunoreactivity

was determined. Because scFv MOC31 was found to be completely inactive after overnight incubation, earlier time points were included in the measurement. Already after 1 h, the activity had dropped to $6.32 \pm 0.2\%$ (9.4% of the initial immunoreactivity). After 4 h, only $2.0 \pm 0.2\%$ (2.9%) remained active. In contrast, the activity of 4D5 MOC-A dropped to $8.1 \pm 4.7\%$ (17.1% of the initial value) over 20 h, that of scFv 4D5 MOC-B to $36 \pm 1.6\%$ (48.3%), and that of scFv 4D5 to $40.5 \pm 8.8\%$ (46.3%), confirming the different thermal stabilities found in the gel filtration assay.

Blood Clearance and Tumor Localization. Diagnostic and therapeutic potential of antibody fragment depends on their rapid blood clearance and quantitative tumor localization. To demonstrate the different targeting efficacy of the various $^{99\text{m}}\text{Tc}$ -labeled scFv fragments, biodistribution studies were performed. For scFv MOC31, we were unable to measure a tumor: blood ratio >0.92 after 1 h, 4 h, and

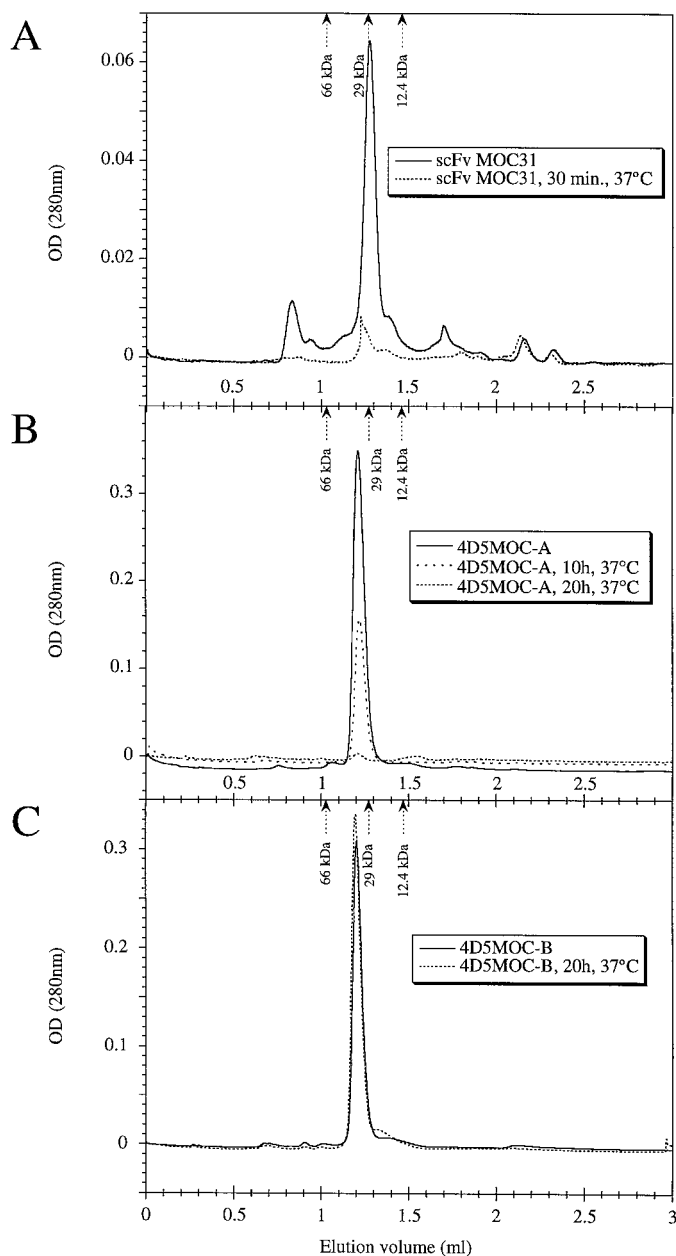


Fig. 4. Thermal stability of scFv fragments. Gel filtration analysis of scFvMOC31 (A), 4D5 MOC-A (B), and 4D5 MOC-B (C) on a Superdex-75 column before and after incubation at 37°C for different time periods. Note the different O. D. scale.

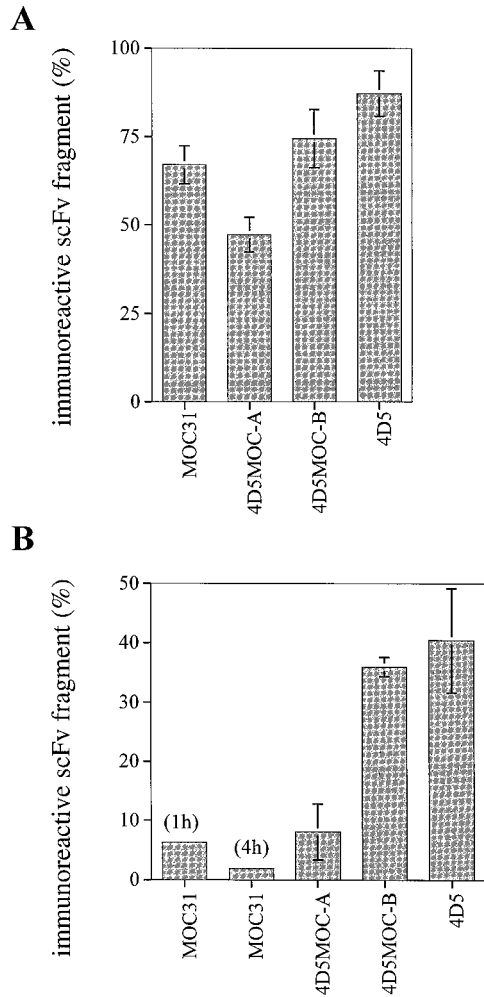


Fig. 5. Serum stability of scFv fragments. Immunoreactivity of ^{99m}Tc -labeled scFv fragments before (A) and after overnight incubation (20 h; B) in human serum at 37°C .

24 h ($n = 3$ for each time point). After 24 h, the total dose in the tumor was 1.24% ID/g compared to 1.34% ID/g in the blood. The blood values were 3–5-fold higher than usually observed after 24 h with this labeling method (Table 2), suggesting binding to serum components such as albumin. In contrast, the biodistribution of ^{99m}Tc -labeled scFv 4D5 revealed a tumor:blood ratio of 8.3 and a total dose of 1.5% ID/g in SK-OV-3 tumor xenografts after 24 h (39). Similar results were also reported for the anti-*c-erbB2* scFv C6.5 (48). Whereas 4D5

MOC-A accumulated only marginally after 24 h in the tumor xenograft with a total dose of 0.84% ID/g and a tumor:blood ratio of 1.95 (Table 3), injection of 4D5 MOC-B in SW2 tumor-bearing mice resulted in a tumor:blood ratio of 5.25 and a total dose of 1.47% ID/g after 24 h. The maximum dose measured at the tumor was 1.82% ID/g after 4 h, which then slowly decreased, reflecting the fast and stable binding of scFv 4D5 MOC-B to the tumor cells (Table 3). For the nonspecific antiluorescein control scFv FITC-E2 (18), no accumulation at the tumor site was detected (Tables 2 and 3).

Clearance studies revealed scFv 4D5 MOC-B to be rapidly cleared with a $t_{1/2\alpha} = 6$ min and $t_{1/2\beta} = 228$ min. The comparison with scFv 4D5 ($t_{1/2\alpha} = 7.5$ min) shows that the clearing behavior, which is a prerequisite for the achievement of high tumor-to-blood-ratios, was not lost during the loop grafting procedure.

DISCUSSION

Biophysical properties of recombinant antibodies are not usually examined, but when they are, problems appear to occur not infrequently (12, 18, 49), both in recombinant antibodies obtained from libraries as well as those constructed from hybridomas, clearly limiting the use of such recombinant antibody fragments, even if they have very promising binding properties. In the present study, an antibody scFv fragment directed against the tumor-associated antigen EGP-2 was produced by cloning the variable domains of the murine hybridoma MOC31 in the scFv fragment format (19). The resulting scFv showed high binding affinity and specificity for EGP-2, a finding which has also been reported by others (41) using immunohistochemical analysis. Initial stability analysis revealed that the MOC31 scFv formed high molecular weight aggregates and rapidly lost its activity when incubated in serum at 37°C (Table 2), and this is also reflected in its lower expression yield. This was due to insufficient thermal stability rather than proteolytic degradation because similar precipitation and loss of immunoreactivity could also be observed upon incubation of highly purified scFv at 37°C in PBS. Not unexpectedly, the scFv fragment failed to significantly enrich at EGP-2-positive lung tumor xenografts in athymic mice and showed significant slower clearance rates than an irrelevant control scFv. However, we wished to develop a general method to overcome such problems.

To improve the biophysical properties of unstable scFv fragments and improve their functional limitation *in vivo*, two approaches have been suggested: (a) *in vitro* evolution toward better thermal stability by combining random mutagenesis with selection for improved functionality at elevated temperature (50) or (b) grafting the antigen binding loops of the scFv fragment onto a scFv framework with more favorable biophysical properties (21). Although the first approach has

Table 3 Biodistribution of ^{99m}Tc -labeled scFvs in athymic mice bearing SW2 tumor xenografts

Organs	4D5MOC-B			4D5MOC-A	FITC-E2
	1 h ($n = 3$)	4 h ($n = 3$)	24 h ($n = 3$)	24 h ($n = 3$)	24 h ($n = 3$)
	ID/g ^a	ID/g	ID/g	ID/g	ID/g
Blood	2.92 ± 0.47	1.31 ± 0.23	0.28 ± 0.06	0.43 ± 0.20	0.17 ± 0.02
Heart	0.97 ± 0.21	0.57 ± 0.11	0.28 ± 0.09	0.63 ± 0.18	0.16 ± 0.04
Lung	3.2 ± 1.29	1.2 ± 0.08	1.14 ± 0.60	1.77 ± 0.95	0.24 ± 0.05
Spleen	0.61 ± 0.06	0.67 ± 0.19	0.7 ± 0.13	1.57 ± 0.44	0.22 ± 0.04
Kidney	120 ± 7	140 ± 4	300 ± 85	90 ± 50	380 ± 60
Stomach	0.48 ± 0.09	0.49 ± 0.1	0.24 ± 0.21	0.26 ± 0.07	0.26 ± 0.13
Intestine	1.33 ± 0.64	0.71 ± 0.06	0.30 ± 0.07	0.48 ± 0.15	0.21 ± 0.07
Liver	6.49 ± 1.53	6.86 ± 0.32	2.38 ± 0.52	4.37 ± 1.87	1.33 ± 0.33
Muscle	0.27 ± 0.01	0.17 ± 0.03	0.1 ± 0.02	0.21 ± 0.09	0.07 ± 0.01
Bone	0.29 ± 0.21	0.21 ± 0.16	0.06 ± 0.05	0.25 ± 0.31	0.06 ± 0.05
Tumor	1.74 ± 0.51	1.82 ± 0.22	1.47 ± 0.32	0.84 ± 0.38	0.23 ± 0.04
Tumor:blood ratio ^b	0.59	1.38	5.25	1.95	1.35

^a Biodistribution of ^{99m}Tc -labeled scFv MOC31 and FITC-E2 was studied in athymic mice bearing SW2 tumors of 40–80 mg in size after i.v. injection of the radiolabeled antibodies. Data are expressed as the mean ± SD.

^b The ratios presented are the averages of the tumor:blood ratios for the individual mice.

been successfully used in our laboratory to achieve very stable scFv fragments (50), the second approach offers the advantage to humanizing the scFv, if it was murine, by use of human framework sequences as the graft acceptor at the same time.

We have used here the second approach to transferring the EGP-2 binding site of scFv MOC31 to the artificial human consensus framework of scFv 4D5, which essentially corresponds to the germ-line sequences IGVH 3–66 and IGVK 1–39 (IMGT nomenclature)⁴. The successful grafting of CDRs of mAbs for humanization purposes has been reported in numerous studies (summarized in Refs. 12 and 51) and is now considered a standard technology to produce humanized antibody fragments. Particularly, the 4D5 framework could prove to be a suitable acceptor of a variety of CDRs (21, 26, 52).

The presented design of the 4D5-MOC31 chimeric antibody fragment was based on the known X-ray structure of the framework template 4D5 (PDB entry 1fvc). A model of the MOC31 structure was generated by homology modeling. Because no structural data on the EGP-2-MOC31 interaction were available, we decided to preserve all potential antibody-antigen contact residues based on an analysis of all antibody-protein complex structures in the PDB database (A. Honegger, unpublished results). In addition to the “classical” CDR regions, some residues adjacent to the CDRs, as well as residues that determine the conformation of the “outer loops” of both domains, were retained from the MOC31 sequence to preserve the topology of the potential antigen interaction surface. This strategy proved to be successful because both graft variants showed binding characteristics indistinguishable from those of the parent mAb and the scFv (Table 1).

During modeling, we realized that the V_H domain of the framework template 4D5 belongs to a different structural subclass than the loop donor MOC31. Because there are several examples in the literature in which a simple loop graft failed and the chimeric antibody fragments had to be rescued by multiple additional back-mutations (52), we directly designed a second chimeric scFv in which the structural subclass and core packing of MOC31 were retained. This involved the changing of eight additional residues, mostly in the V_H core, to the murine sequence, thereby essentially corresponding to a resurfacing of the MOC31 V_H domain. These additional mutations had no effect on the antigen binding affinity and resulted in an increased stability of the chimeric scFv. Whereas the loop graft 4D5 MOC-A revealed a thermal stability intermediate between that of the two parent scFv 4D5 and MOC31, the additional mutations in 4D5 MOC-B yielded a molecule with similar favorable properties as the framework donor scFv 4D5. This finding was surprising considering the fact that 4D5 MOC-B has less sequence homology to 4D5 than 4D5 MOC-A. It suggests that it may indeed be critical to maintain a framework class as defined by the residues H6, H7, and H9 throughout the grafting and to not mix the framework because these residues are interrelated. Furthermore, although the sequence of 4D5 MOC-B and MOC31 are most closely related, their difference in stability was greatest.

It has recently been shown that the V_L domain of 4D5 is exceptionally stable and that the thermodynamic stability of the 4D5 scFv is limited by intrinsic stability of its V_H domain (49). Grafting of the MOC31 antigen binding surface onto this fragment resulted in a chimeric scFv with intermediate stability. This might be due to unfavorable interactions within the grafted loops or between grafted core residues and to incompatible framework core residues. However, there are only few contact sites between those framework residues in the lower core that differ between 4D5 and MOC31 and core residues from the grafted loops, both being separated by a layer of conserved residues (Fig. 1). The main direct contact site between the residues changed in the loop graft and the group of residues additionally changed in 4D5 MOC-B is located between Met H48 (Val in 4D5) and Phe H63 (Val in 4D5 and in 4D5 MOC-A). If there had been a

steric clash occurring in the original graft, we would have expected aggravation by the substitution of the contact residue with a larger residue. It is therefore more likely that the destabilizing influence of the loops was compensated by a general stabilization of the domain core.

As indicated by the biodistribution data (Tables 2 and 3), the stabilization achieved by the grafting in 4D5 MOC-A and by the additional core mutations in 4D5 MOC-B was crucial for the effective enrichment at the xenografted tumor achieved by reducing the blood clearance of the targeting agent. Because the radiolabel is stably bound to the his-tag (39), the radioactivity determined at the xenografted tumor suggests still rather unsatisfactory tumor localization and retention characteristics of the scFv fragments tested, and these data are very similar to those found for other scFv fragments (11, 39, 48). The moderate localization is probably a consequence of pharmacokinetics, leading to rapid clearance. Further improvements must therefore involve the change in format, notably the use of multivalent constructs (13). However, only by the engineering described here have the appropriate building blocks become available.

The scFv MOC31, which lost most of its antigen binding activity within 1 h at 37°C, did localize to the tumor but cleared more slowly than the control antibody and the grafted constructs from the circulation, never reaching a tumor: blood ratio different from the nonspecific control (total dose, 1.24% ID/g tissue; tumor: blood ratio of 0.92). 4D5 MOC-A, which was stable for several hours at 37°C, revealed only modest tumor accretion (total dose, 0.84% ID/g tissue; tumor: blood ratio of 1.95). For comparison, injection of the most stable construct, 4D5 MOC-B, into animals resulted in 1.47% ID/g tumor tissue, with a tumor: blood ratio of 5.25. We explain the difference in the clearance rates of the molecules with this difference in thermal stability. The aggregation-sensitive scFv MOC31 fragment unfolds rather quickly due to its low thermal stability and exposes hydrophobic patches that can interact either with other unfolded MOC31 molecules or with serum components (e.g., albumin), leading to soluble high-molecular weight aggregates with increased circulation time. Nevertheless, they do not act as a reservoir for further tumor localization because they are irreversibly unfolded. In parallel, we expect the more stable molecules to retain their binding activity on their receptor for longer times and thus remain localized at the tumor site when the blood level decreases. It might be possible that lower thermal stability causes an increase in the effective off-rate from the receptor under *in vivo* conditions because the molecules may denature. For further improvement, the present framework can be further equipped with intermolecular disulfide bonds (53), albeit at the cost of lower production yield, and it can conveniently be transferred into multivalent formats (13) to increase tumor retention.

In a recent study, indium-diethylenetriaminepentaacetic acid-labeled mAb MOC31 was used to detect primary tumors and metastases in patients with small cell lung cancer (4). However, the diagnostic benefit of this approach was not superior to conventional diagnostic techniques such as computer tomography scans. In a preclinical study, an immunotoxin consisting of *Pseudomonas* exotoxin-A, which is chemically linked to mAb MOC31, induced regression of small lung cancer xenografts in athymic mice but could only delay the growth of larger tumors. This finding suggests insufficient tumor penetration to limit the antitumor activity (5). Reduction in size might help to increase the therapeutic efficacy of immunotoxins and other immunconjugates. Moreover, the improved scFv can now also serve as a building block for other recombinant molecules such as dimeric and multimeric miniantibodies (13) and Fab or (Fab)₂ to optimize size and avidity effects. The unstable parent scFv MOC31 has also been used for the construction of a EGP-2/CD3 diabody for T-cell retargeting to tumor cells (54). Interestingly, in this format, the scFv was reported to

show sufficient immunoreactivity with a half-life of 12 h at 37°C in human serum, but the production yield was as low as for scFv MOC31 presented in our study. *In vivo* data on the diabody have not been reported thus far.

In this study, we demonstrate the importance of engineering for folding and stability to improve the biophysical properties of antibody fragments of potential clinical benefit. As an example, an unstable and poorly expressing murine anti-EGP-2 scFv, which failed to target specifically to tumors *in vivo*, was converted to a well-expressing and very stable humanized antibody fragment with the same antigen specificity. This novel rationally engineered scFv efficiently enriched to EGP-2-positive lung tumor xenografts in athymic mice and can serve as an promising building block for more advanced recombinant antibodies and fusions with tailor-made targeting properties. We believe that engineering for folding and stability of recombinant molecules, whether derived from libraries or hybridomas, is of outstanding benefit for the development of antibodies and fusion proteins for enhanced diagnostic and therapeutic efficacy.

ACKNOWLEDGMENTS

We thank Christine de Pasquale for excellent technical assistance and Drs. Ilse Novak-Hofer, Alain Tissot, Gerd Lüdke, and Hendrick Bothmann for helpful discussions.

REFERENCES

- De Leij, L., Helfrich, W., Stein, R., and Mattes, M. J. SCLC-cluster-2 antibodies detect the pancarcinoma/epithelial glycoprotein EGP-2. *Int. J. Cancer Suppl.*, 8: 60–63, 1994.
- Riethmüller, G., Schneider-Gädick, E., Schlimok, G., Schmiegel, W., Raab, R., Hoffken, K., Gruber, R., Pichlmaier, H., Hirche, H., Pichlmayr, R. Randomised trial of monoclonal antibody for adjuvant therapy of resected Dukes' C colorectal carcinoma. German Cancer Aid 17–1A Study Group. *Lancet*, 343: 1177–1183, 1994.
- Elias, D. J., Hirschowitz, L., Kline, L. E., Kroener, J. F., Dillman, R. O., Walker, L. E., Robb, J. A., and Timms, R. M. Phase I clinical comparative study of monoclonal antibody KS1/4 and KS1/4-methotrexate immunocjugate in patients with non-small cell lung carcinoma. *Cancer Res.*, 50: 4154–4159, 1990.
- Kosterink, J. G., de Jonge, M. W., Smit, E. F., Piers, D. A., Kengen, R. A., Postmus, P. E., Shochat, D., Groen, H. J., The, H. T., and de Leij, L. Pharmacokinetics and scintigraphy of indium-111-DTPA-MOC-31 in small-cell lung carcinoma. *J. Nucl. Med.*, 36: 2356–2362, 1995.
- Zimmermann, S., Wels, W., Froesch, B. A., Gerstmayer, B., Stahel, R. A., and Zangemeister-Wittke, U. A novel immunotoxin recognising the epithelial glycoprotein-2 has potent antitumoural activity on chemotherapy-resistant lung cancer. *Cancer Immunol. Immunother.*, 44: 1–9, 1997.
- Litvinov, S. V., Velders, M. P., Bakker, H. A., Fleuren, G. J., and Warnaar, S. O. Ep-CAM: a human epithelial antigen is a homophilic cell-cell adhesion molecule. *J. Cell. Biol.*, 125: 437–446, 1994.
- Cirulli, V., Crisa, L., Beattie, G. M., Mally, M. I., Lopez, A. D., Fannon, A., Ptasznik, A., Inverardi, L., Ricordi, C., Deerinck, T., Ellisman, M., Reisfeld, R. A., and Hayek, A. KSA antigen Ep-CAM mediates cell-cell adhesion of pancreatic epithelial cells: morphoregulatory roles in pancreatic islet development. *J. Cell. Biol.*, 140: 1519–1534, 1998.
- Basak, S., Speicher, D., Eck, S., Wunner, W., Maul, G., Simmons, M. S., and Herlyn, D. Colorectal carcinoma invasion inhibition by CO17–1A/GA733 antigen and its murine homologue. *J. Natl. Cancer Inst.*, 90: 691–697, 1998.
- Huston, J. S., McCartney, J., Tai, M. S., Mottola-Hartshorn, C., Jin, D., Warren, F., Keck, P., and Oppermann, H. Medical applications of single-chain antibodies. *Int. Rev. Immunol.*, 10: 195–217, 1993.
- Wels, W., Harwerth, I. M., Mueller, M., Groner, B., and Hynes, N. E. Selective inhibition of tumor cell growth by a recombinant single-chain antibody-toxin specific for the erbB-2 receptor. *Cancer Res.*, 52: 6310–6317, 1992.
- Begent, R. H., Verhaar, M. J., Chester, K. A., Casey, J. L., Green, A. J., Napier, M. P., Hope-Stone, L. D., Cushen, N., Keep, P. A., Johnson, C. J., Hawkins, R. E., Hilson, A. J., and Robson, L. Clinical evidence of efficient tumor targeting based on single-chain Fv antibody selected from a combinatorial library. *Nat. Med.*, 2: 979–984, 1996.
- Carter, P., and Merchant, A. M. Engineering antibodies for imaging and therapy. *Curr. Opin. Biotechnol.*, 8: 449–454, 1997.
- Plückthun, A., and Pack, P. New protein engineering approaches to multivalent and bispecific antibody fragments. *Immunotechnology*, 3: 83–105, 1997.
- Bird, R. E., Hardman, K. D., Jacobson, J. W., Johnson, S., Kaufman, B. M., Lee, S. M., Lee, T., Pope, S. H., Riordan, G. S., and Whitlow, M. Single-chain antigen-binding proteins. *Science (Washington DC)*, 242: 423–426, 1988.
- Huston, J. S., Levinson, D., Wadgett-Hunter, M., Tai, M. S., Novotny, J., Margolies, M. N., Ridge, R. J., Brucoleri, R. E., Haber, E., Crea, R. Protein engineering of antibody binding sites: recovery of specific activity in an anti-digoxin single-chain Fv analogue produced in *Escherichia coli*. *Proc. Natl. Acad. Sci. USA*, 85: 5879–5883, 1988.
- Skerra, A., and Plückthun, A. Assembly of a functional immunoglobulin Fv fragment in *Escherichia coli*. *Science (Washington DC)*, 240: 1038–1041, 1988.
- Winter, G., Griffiths, A. D., Hawkins, R. E., and Hoogenboom, H. R. Making antibodies by phage display technology. *Annu. Rev. Immunol.*, 12: 433–455, 1994.
- Vaughan, T. J., Williams, A. J., Pritchard, K., Osbourn, J. K., Pope, A. R., Earnshaw, J. C., McCafferty, J., Hodits, R. A., Wilton, J., and Johnson, K. S. Human antibodies with sub-nanomolar affinities isolated from a large non-immunized phage display library. *Nat. Biotechnol.*, 14: 309–314, 1996.
- Krebber, A., Bornhauser, S., Burmester, J., Honegger, A., Willuda, J., Bosshard, H. R., and Plückthun, A. Reliable cloning of functional antibody variable domains from hybridomas and spleen cell repertoires employing a reengineered phage display system. *J. Immunol. Methods*, 201: 35–55, 1997.
- Dall'Acqua, W., and Carter, P. Antibody engineering. *Curr. Opin. Struct. Biol.*, 8: 443–450, 1998.
- Jung, S., and Plückthun, A. Improving *in vivo* folding and stability of a single-chain Fv antibody fragment by loop grafting. *Protein Eng.*, 10: 959–966, 1997.
- Carter, P., Presta, L., Gorman, C. M., Ridgway, J. B., Henner, D., Wong, W. L., Rowland, A. M., Kotts, C., Carver, M. E., and Shepard, H. M. Humanization of an anti-p185HER2 antibody for human cancer therapy. *Proc. Natl. Acad. Sci. USA*, 89: 4285–4289, 1992.
- Carter, P., Kelley, R. F., Rodrigues, M. L., Snedecor, B., Covarrubias, M., Velligan, M. D., Wong, W. L., Rowland, A. M., Kotts, C. E., Carver, M. E. High level *Escherichia coli* expression and production of a bivalent humanized antibody fragment. *Biotechnology (NY)*, 10: 163–167, 1992.
- Wörn, A., and Plückthun, A. An intrinsically stable antibody scFv fragment can tolerate the loss of both disulfide bonds and fold correctly. *FEBS Lett.*, 427: 357–361, 1998.
- Helfrich, W., Koning, P. W., The, T. H., and De Leij, L. Epitope mapping of SCLC-cluster-2 MAb and generation of antibodies directed against new EGP-2 epitopes. *Int. J. Cancer Suppl.*, 8: 64–69, 1994.
- Knappik, A., and Plückthun, A. Engineered turns of a recombinant antibody improve its *in vivo* folding. *Protein Eng.*, 8: 81–89, 1995.
- Pokkuluri, P. R., Bouthillier, F., Li, Y., Kuderova, A., Lee, J., and Cygler, M. Preparation, characterization, and crystallization of an antibody Fab fragment that recognizes RNA. Crystal structures of native Fab and three Fab-monomucleotide complexes. *J. Mol. Biol.*, 243: 283–297, 1994.
- Tulip, W. R., Varghese, J. N., Webster, R. G., Laver, W. G., and Colman, P. M. Crystal structures of two mutant neuraminidase-antibody complexes with amino acid substitutions in the interface. *J. Mol. Biol.*, 227: 149–159, 1992.
- Tulip, W. R., Varghese, J. N., Laver, W. G., Webster, R. G., and Colman, P. M. Refined crystal structure of the influenza virus N9 neuraminidase-NC41 Fab complex. *J. Mol. Biol.*, 227: 122–148, 1992.
- Colman, P. M., Laver, W. G., Varghese, J. N., Baker, A. T., Tulloch, P. A., Air, G. M., and Webster, R. G. Three-dimensional structure of a complex of antibody with influenza virus neuraminidase. *Nature (Lond.)*, 326: 358–363, 1987.
- Shoham, M. Crystal structure of an anticholera toxin peptide complex at 2.3 Å. *J. Mol. Biol.*, 232: 1169–1175, 1993.
- Shoham, M., Proctor, P., Hughes, D., and Baldwin, E. T. Crystal parameters and molecular replacement of an anticholera toxin peptide complex. *Proteins*, 11: 218–222, 1991.
- Eigenbrot, C., Randal, M., Presta, L., Carter, P., and Kossiakoff, A. A. X-ray structures of the antigen-binding domains from three variants of humanized anti-p185HER2 antibody 4D5 and comparison with molecular modeling. *J. Mol. Biol.*, 229: 969–995, 1993.
- Prodromou, C., and Pearl, L. H. Recursive PCR: a novel technique for total gene synthesis. *Protein Eng.*, 5: 827–829, 1992.
- Ge, L., Knappik, A., Pack, P., Freund, C., and Plückthun, A. Expressing Antibodies in *Escherichia coli*. In: C. A. K. Borrebaeck (ed.), *Antibody Engineering*, 2nd ed., pp. 229–261. Oxford, United Kingdom: Oxford University Press, 1995.
- Tang, Y., Jiang, N., Parakh, C., and Hilvert, D. Selection of linkers for a catalytic single-chain antibody using phage display technology. *J. Biol. Chem.*, 271: 15682–15686, 1996.
- Bass, S., Gu, Q., and Christen, A. Multicopy suppressors of prc mutant *Escherichia coli* include two HtrA (DegP) protease homologs (HhoAB), DksA, and a truncated RlpA. *J. Bacteriol.*, 178: 1154–1161, 1996.
- Plückthun, A., Krebber, A., Krebber, C., Horn, U., Knüpfer, U., Wenderoth, R., Niebla, L., Proba, K., and Riensenberg, D. Producing antibodies in *Escherichia coli*: from PCR to fermentation. In: B. D. Hames (ed.), *Antibody Engineering*, pp. 203–249. Oxford, United Kingdom: Oxford University Press, 1996.
- Waibel, R., Alberto, R., Willuda, J., Finern, R., Schibli, R., Stichelberger, A., Egli, A., Abram, U., Mach, J.-P., Plückthun, A., and Schubiger, P. A. Stable one-step technetium-99m labeling of His-tagged recombinant proteins with a novel Tc (I)-carbonyl complex. *Nat. Biotechnol.*, 17: 897–901, 1999.
- Lindmo, T., Boven, E., Cuttiita, F., Fedorko, J., and Bunn, P. A., Jr. Determination of the immunoreactive fraction of radiolabeled monoclonal antibodies by linear extrapolation to binding at infinite antigen excess. *J. Immunol. Methods*, 72: 77–89, 1984.
- Roovers, R. C., Henderikx, P., Helfrich, W., van der Linden, E., Reurs, A., de Bruine, A. P., Arends, J. W., de Leij, L., and Hoogenboom, H. R. High-affinity recombinant phage antibodies to the pan-carcinoma marker epithelial glycoprotein-2 for tumour targeting. *Br. J. Cancer*, 78: 1407–1416, 1998.
- Holm, L., and Sander, C. The FSSP database: fold classification based on structure-structure alignment of proteins. *Nucl. Acids Res.*, 24: 206–209, 1996.

43. Kabat, E. A., Wu, T. T., Perry, H. M., Gottesman, K. S., and Foeller, C. Sequences of Proteins of Immunological Interest, 5th ed. Bethesda, MD: United States Department of Health and Human Services, Public Health Service, and NIH, 1991.
44. Chothia, C., and Lesk, A. M. The relation between the divergence of sequence and structure in proteins. *EMBO J.*, 5: 823–826, 1986.
45. Saul, F. A., and Poljak, R. J. Structural patterns at residue positions 9, 18, 67, and 82 in the VH framework regions of human and murine immunoglobulins. *J. Mol. Biol.*, 230: 15–20, 1993.
46. Langedijk, A. C., Honegger, A., Maat, J., Planta, R. J., van Schaik, R. C., and Plückthun, A. The nature of antibody heavy chain residue H6 strongly influences the stability of a VH domain lacking the disulfide bridge. *J. Mol. Biol.*, 283: 95–110, 1998.
47. Bothmann, H., and Plückthun, A. Selection for a periplasmic factor improving phage display and functional periplasmic expression. *Nat. Biotechnol.*, 16: 376–380, 1998.
48. Adams, G. P., Schier, R., Marshall, K., Wolf, E. J., McCall, A. M., Marks, J. D., and Weiner, L. M. Increased affinity leads to improved selective tumor delivery of single-chain Fv antibodies. *Cancer Res.*, 58: 485–490, 1998.
49. Wörn, A., and Plückthun, A. Different equilibrium stability behavior of scFv fragments: identification, classification, and improvement by protein engineering. *Biochemistry*, in press, 1999.
50. Proba, K., Wörn, A., Honegger, A., and Plückthun, A. Antibody scFv fragments without disulfide bonds made by molecular evolution. *J. Mol. Biol.*, 275: 245–253, 1998.
51. Winter, G., and Harris, W. J. Humanized antibodies. *Trends Pharmacol. Sci.*, 14: 139–143, 1993.
52. Baca, M., Presta, L. G., O'Connor, S. J., and Wells, J. A. Antibody humanization using monovalent phage display. *J. Biol. Chem.*, 272: 10678–10684, 1997.
53. Young, N. M., MacKenzie, C. R., Narang, S. A., Oomen, R. P., and Baenziger, J. E. Thermal stabilization of a single-chain Fv antibody fragment by introduction of a disulphide bond. *FEBS Lett.*, 377: 135–137, 1995.
54. Helfrich, W., Kroesen, B. J., Roovers, R. C., Westers, L., Molema, G., Hoogenboom, H. R., and de Leij, L. Construction and characterization of a bispecific diabody for retargeting T cells to human carcinomas. *Int. J. Cancer*, 76: 232–239, 1998.